Journal of Zhejiang University SCIENCE
ISSN 1009-3095
http://www.zju.edu.cn/jzus
E-mail: jzus@zju.edu.cn

Physical modelling and scale effects of air-water flows on stepped spillways*

CHANSON Hubert†, GONZALEZ Carlos A.
(*Department of Civil Engineering, The University of Queensland, Brisbane 4072, Australia*)
†E-mail: h.chanson@uq.edu.au

Received Apr. 1, 2004; revision accepted Jan. 20, 2005

Abstract: During the last three decades, the introduction of new construction materials (e.g. RCC (Roller Compacted Concrete), strengthened gabions) has increased the interest for stepped channels and spillways. However stepped chute hydraulics is not simple, because of different flow regimes and importantly because of very-strong interactions between entrained air and turbulence. In this study, new air-water flow measurements were conducted in two large-size stepped chute facilities with two step heights in each facility to study experimental distortion caused by scale effects and the soundness of result extrapolation to prototypes. Experimental data included distributions of air concentration, air-water flow velocity, bubble frequency, bubble chord length and air-water flow turbulence intensity. For a Froude similitude, the results implied that scale effects were observed in both facilities, although the geometric scaling ratio was only L_r=2 in each case. The selection of the criterion for scale effects is a critical issue. For example, major differences (i.e. scale effects) were observed in terms of bubble chord sizes and turbulence levels although little scale effects were seen in terms of void fraction and velocity distributions. Overall the findings emphasize that physical modelling of stepped chutes based upon a Froude similitude is more sensitive to scale effects than classical smooth-invert chute studies, and this is consistent with basic dimensional analysis developed herein.

Key words: Physical modelling, Scale effects, Stepped spillways, Air entrainment, Air-water flow measurements
doi:10.1631/jzus.2005.A0243 **Document code:** A **CLC number:** TU411

INTRODUCTION

The stepped channel design has been used for more than 3500 years. Greek and Minoan engineers were probably the first to design an overflow stepped weir and stepped storm waterways respectively (Chanson, 2001). Later, Roman, Moslem, Mughal and Spanish designers used a similar technique. The steps increase significantly the rate of energy dissipation taking place on the channel face, reducing the size of the required downstream energy dissipation and the risks of scouring. Recently, new construction materials (e.g. RCC, strengthened gabions) have increased the interest for stepped channels and spillways. The construction of stepped chutes is compatible with the slipforming and placing methods of roller compacted concrete, with the construction techniques of gabion dams and with debris flow conveyance technique (Fig.1). During the last three decades, research in the hydraulics of stepped spillways has been very active with 2 books, 2 international workshops and over 35 international refereed journal articles (Ohtsu and Yasuda, 1998; Minor and Hager, 2000; Chanson, 2001). This was associated with the completion of the world's largest stepped spillways, in terms of design discharge capacity: e.g., Shuidong and Dachaoshan dams (Lin and Han, 2001).

For a given stepped chute, waters flow as a succession of free-falling nappes (nappe flow regime) at small discharges (Chanson, 1994; Chamani and Rajaratnam, 1994; Toombes, 2002). For an intermediate range of flow rates, a transition flow regime is observed (Chanson and Toombes, 2004). Most prototype spillways operate at large discharges per unit width (i.e. skimming flow regime) for which the wat-

* Project supported by the National Council for Science and Technology of Mexico (CONACYT)

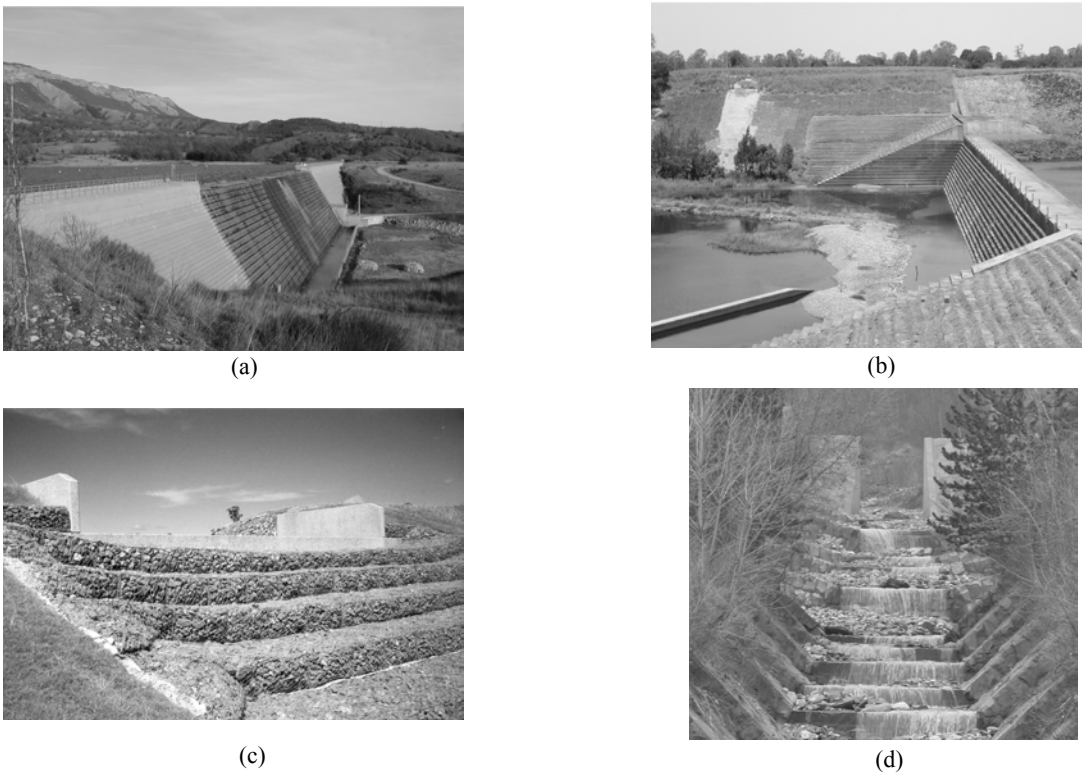

(a) (b) (c) (d)

Fig.1 Examples of stepped spillways and waterways

(a) Riou dam stepped spillway (France) on 11 Feb. 2004. Completed in 1990, the 22 m high RCC dam is part of a hydropower scheme. Stepped chute characteristics: h=0.43 m, θ=59°, W=96 m, q_{des}=1.15 m^2/s; (b) Bucca weir (Australia) on 23 Dec. 2001. Irrigation water supply for sugar cane. Stepped chute characteristics: h=0.6 m, θ=63.4°, W=130.8 m, q_{des}=55.4 m^2/s. Note the tilting splitters installed at the crest to aerate the deflected nappe at low flows, reducing noise and vibrations to the structure; (c) Gabion stepped weir at Robina, Gold Coast (Australia) on 2 Apr. 1997, shortly after completion. Stepped weir characteristics: h=0.6 m, W=10.5 m, Reno mattress construction; (d) Artificial stepped waterway along Ruisseau Ravin de St Julien, in St-Julien-Mont-Denis (France), on 11 Feb. 2004. Looking upstream with a slit check dam in background, the waterway is designed to carry safely debris flow around the township

ers skim as a coherent stream over the pseudo-bottom formed by step edges (Figs.2 and 3). Skimming flows are characterized by very-significant form losses and momentum transfer from the main stream to the recirculation zones (Chanson *et al*., 2002). There is an obvious analogy with skimming flows past large elements and boundary layer flows past *d*-type roughness (Knight and Macdonald, 1979; Djenidi *et al*., 1999).

Stepped chute hydraulics is not simple, because of different flow regimes, but most importantly because of strong flow aeration, very-strong turbulence, and interactions between entrained air and turbulence (Chanson and Toombes, 2002). To date, little research was conducted at the microscopic scale on the complex nature of the flow and its physical modelling. It is the purpose of this study to discuss similitude and scale effects affecting stepped chute flows. The analysis is supported by a series of systematic measurements conducted in two large-size facilities with two step sizes each. The geometric scaling ratio was L_r=2 in each case. The results provide a new understanding of scale effects affecting stepped chute flows.

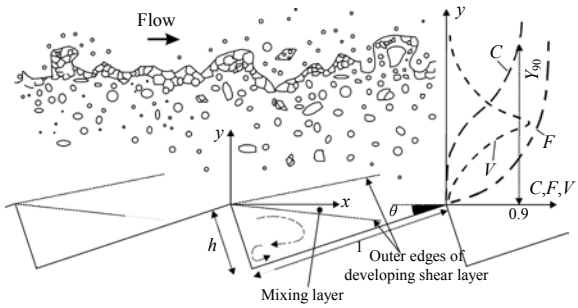

Fig.2 Skimming flow over a stepped chute: definition sketch

(a)

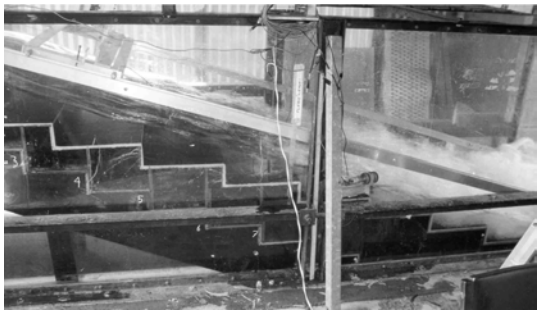

(b)

Fig.3 Photographs of skimming flows in Channel 2
(a) h=0.05 m, d_c/h=1.7; (b) h=0.10 m, d_c/h=1.53

DIMENSIONAL ANALYSIS AND SIMILITUDE

Basic analysis

A dominant characteristic of stepped chute flows is the strong flow aeration ('white waters') clearly seen in prototype and laboratory (Fig.3). Theoretical analysis (and numerical study) is limited considering the large number of relevant equations: i.e., three basic equations per phase plus a phase transfer equation. Experimental investigations are also difficult but recent advances in air-water flow instrumentation brought new measuring systems enabling successful experiments (Chanson, 2002).

Traditionally model studies are performed with geometrically similar models and the geometric scaling ratio L_r is defined as the ratio of prototype to model dimensions. Laboratory studies of air-water flows require however the selection of an adequate similitude.

The relevant parameters needed for any dimensional analysis include the fluid properties and physical constants, the channel geometry and inflow conditions, the air-water flow properties including the entrained air bubble characteristics, and the geometry of the steps. Considering a skimming flow down a stepped chute with flat horizontal steps at uniform equilibrium and for a prismatic rectangular channel, a complete dimensional analysis yields a relationship between the local air-water flow properties, and the fluid properties, physical constants, flow conditions and step geometry:

$$C, \frac{V}{\sqrt{gd}}, \frac{u'}{V}, \frac{d_{ab}}{d}, \ldots = F_1\left[\frac{x}{d}; \frac{y}{d}; \frac{q_w}{\sqrt{gd^3}}; \rho_w \frac{q_w}{\mu_w}; \frac{g\mu_w^4}{\rho_w \sigma^3}; \frac{d}{h}; \frac{W}{h}; \theta; \frac{k_s'}{h}\right] \quad (1)$$

where C is the local void fraction; V is the local velocity; g is the gravity acceleration; d is the equivalent water depth at uniform equilibrium; u' is a characteristic turbulent velocity; d_{ab} is a characteristic size of entrained bubble; x is the coordinate in the flow direction measured from a step edge; y is the distance normal from the pseudo-bottom formed by the step edges; q_w is the water discharge per unit width; ρ_w and μ_w are the water density and dynamic viscosity respectively; σ is the surface tension between air and water; W is the chute width; h is the step height; θ is the angle between the pseudo-bottom and the horizontal, and k_s' the skin roughness height (Fig.2). For air-water flows, the equivalent clear water depth is defined as:

$$d = \int_{y=0}^{y=Y_{90}} (1-C)\mathrm{d}y \quad (2)$$

where Y_{90} is the depth where C=0.9. In Eq.(1) right hand side, the 3rd, 4th and 5th dimensionless terms are Froude, Reynolds and Morton numbers respectively, and the last four terms characterize the step cavity shape and the skin friction effects on the cavity wall. Note that any combination of dimensionless numbers is also dimensionless. One parameter among the Froude, Reynolds and Weber numbers may be replaced by the Morton number $Mo=(g\mu_w^4)/(\rho_w\sigma^3)$ as seen in Eq.(1) where the Weber number was replaced.

Further simplifications may be derived by considering the depth-averaged air-water flow properties. For a skimming flow at uniform equilibrium, Eq.(1) yields:

$$F_2\left[\frac{U_w}{\sqrt{gd}};\rho_w\frac{U_w d}{\mu_w};\frac{g\mu_w^4}{\rho_w\sigma^3};C_{mean};\frac{d}{h};\frac{W}{h};\theta;\frac{k'_s}{h}\right]=0 \quad (3)$$

where U_w is the mean flow velocity ($U_w=q_w/d$) and C_{mean} is the depth-averaged void fraction:

$$C_{mean}=\frac{1}{Y_{90}}\int_{y=0}^{y=Y_{90}} C\,dy \quad (4)$$

In free-surface flows, most laboratory studies are based upon a Froude similitude (Henderson, 1966; Chanson, 2004). But cavity recirculation and momentum exchanges between cavity and stream flow are dominated by viscous effects suggesting the need for a Reynolds similitude, while the entrapment of air bubbles and the mechanisms of air bubble breakup and coalescence are dominated by surface tension effects implying the need for a Weber similitude. For geometrically-similar models, it is impossible to satisfy simultaneously Froude, Reynolds and Weber similarities unless L_r=1. In small size models (L_r>>1), the air entrainment process may be affected by significant scale effects. Wood (1991) and Chanson (1997) presented comprehensive reviews. Kobus (1984) illustrated some applications.

Despite very simplistic assumptions, Eq.(1), and even Eq.(3), demonstrate that dynamic similarity of stepped chute flows is impossible with geometrically similar models, unless working at full-scale, because of the large number of relevant parameters. Note that, usually, the same fluids (air and water) are used in model and prototype, and the Morton number becomes an invariant.

Discussion

Few studies tested systematically the validity of a Froude similitude with geometric similarity using same fluids in model and prototype (Table 1). These were based upon a Froude similitude with undistorted geometric scale and sometimes two-dimensional models. Results are summarized in Table 1 (Column 3) indicating conditions to avoid scale effects.

BaCaRa (1991) described a systematic laboratory investigation of M'Bali dam spillway with model scales of L_r=10, 21.3, 25 and 42.7. (No protoype test was conducted.) For the smallest models (L_r=25 and 42.7), the flow resistance was improperly reproduced. Chanson *et al*.(2002) re-analyzed more than 38 model studies and 4 prototype investigations with channel slopes ranging from 5.7° up to 55°, and with Reynolds numbers between 3E+4 and 2E+8. They concluded that physical modelling of flow resistance may be conducted based upon a Froude similitude if laboratory flow conditions satisfy h>0.020 m and Re>1E+5. They added that true similarity of air entrainment was achieved only for model scales L_r<10. However detailed studies of local air-water flow properties, including present results, yielded more stringent conditions suggesting the impossibility to achieve dynamic similarity, even in large-size models (Table 1). In the present study, a Froude similitude was used as for most open channel flow studies and past studies.

Table 1 Summary of systematic studies on stepped chute flows based upon a Froude similitude

Study	Definition of scale effects	Limiting conditions to avoid scale effects	Experimental flow conditions
BaCaRa (1991)	Flow resistance and energy dissipation	L_r<25	Model studies: θ=53.1°, h=0.06, 0.028, 0.024, 0.014 m, L_r=10, 21.3, 25, 42.7
Boes (2000)	Void fraction and velocity distributions	Re>1E+5	Model studies: θ=30° and 50°, W=0.5 m, h=0.023 to 0.093 m, L_r=6.6, 13, 26 (30°)/6.5, 20 (50°)
Chanson *et al*. (2002)	Flow resistance	Re>1E+5 h>0.02 m	Prototype and model studies: θ=5° to 50°, W=0.2 to 15 m, h=0.005 to 0.3 m, 3E+4<Re<2E+8, 32<We<6.5E+6
Present study	Void fraction and bubble count rate distributions	L_r<2	θ=3.4°, W=0.5 m, h=0.143, 0.0715 m, 2.4E+5<Re<6E+5, L_r=1, 2
	Void fraction, bubble count rate, velocity and turbulence level distributions, Bubble sizes and clustering	L_r<2	θ=16°, W=1 m, h=0.10, 0.05 m, 1.2E+5<Re<1.2E+6, L_r=1, 2

h: step height; L_r: geometric scaling ratio; $Re=VD_H/\nu_w$; D_H: hydraulic diameter; ν_w: kinematic viscosity of water; W: chute width; $We=\rho_w V^2 d/\sigma$;

EXPERIMENTAL SETUP

Presentation

Experiments were performed in two facilities with flat horizontal steps (Table 2). The first channel was 24 m long, 0.5 m wide with a 3.4° slope. Two step sizes were used: h=0.143 and 0.0715 m. In both cases, the first drop was located 2.4 m downstream of a smooth nozzle (d_n=0.03 m). The channel invert, upstream of the vertical drop, was flat and horizontal for all experiments. Water was supplied by a pump, with a variable-speed electronic controller (Taian™ T-verter K1-420-M3 adjustable frequency AC motor drive), enabling an accurate discharge adjustment in a closed-circuit system. The flow rates were measured with a Dall™ tube flowmeter, calibrated on site. The accuracy of the discharge measurement was approximately 2%.

The second channel was 1 m wide with a 15.9° slope. It consisted of a broad-crest followed by identical steps with two sizes: h=0.1 and 0.05 m (Fig.3). The flow rate was delivered by a pump controlled with an adjustable frequency AC motor drive, enabling an accurate discharge adjustment in a closed-circuit system. The discharge was measured from the upstream head above crest with an accuracy of about 2%, after complete calibration on the crest profile on-site.

Air-water flow properties were measured using a single-tip resistivity probe (∅=0.35 mm) in Channel 1 and a double-tip probe (∅=0.025 mm) in Channel 2. Both probes were developed at the University of Queensland and excited by an air bubble detector (AS25240). The probe signal was scanned at 5 kHz for 60 to 180 s in Channel 1, and at 20 kHz per sensor for 20 s in Channel 2. The translation of the probes in the direction normal to the channel invert was controlled by a fine adjustment travelling mechanism connected to a Mitutoyo™ digimatic scale unit (Ref. No. 572-503). The error on the vertical position of the probe was less than 0.025 mm. Flow visualisations were further conducted with a digital video-camera and high-shutter speed still photographs.

Signal processing and data analysis

The probe signal outputs were post-processed using the method outlined by Chanson (2002) and Chanson and Toombes (2002). A summary follows.

The basic probe outputs are the void fraction, bubble count rate and bubble chord time distributions with both single-tip and double-tip probes. The void fraction C is the proportion of time that the probe tip is in the air. The bubble count rate F is the number of bubbles impacting the probe tip per second. The bubble chord times provide information on the air-water flow structure.

With a dual-tip probe, the velocity measurement is based upon the successive detection of air-water interfaces by two sensors. In turbulent air-water flows, the successive detection of all bubbles by each tip is highly improbable and it is common to use a cross-correlation technique. The time-averaged air-water velocity is $V=\Delta x/T$, where Δx is the distance between tips and T is the time for which the cross-correlation function R_{xy} is maximum. The shape of the cross-correlation function provides further information on the velocity fluctuations (Chanson and Toombes, 2002). The turbulent intensity may be derived from the broadening of the cross-correlation function compared to the auto-correlation function:

$$Tu=\frac{u'}{V}=0.851\frac{\sqrt{\Delta T^2-\Delta t^2}}{T} \tag{5}$$

Table 2 Summary of experimental flow conditions

Reference	θ (°)	q_w (m^2/s)	h (m)	d_c/h	Flow regime	Instrumentation	Remarks
Channel 1	3.4				Transition flow	Single-tip conductivity probe (∅=0.35 mm)	L=24 m, W=0.5 m Inflow: pressurised intake
		0.150	0.143	0.92			Experiments CR98
		0.06	0.0715	1.0			Experiments EV200
		0.08		1.2			
Channel 2	15.9			0.85~1.7	Transition and skimming flows	Double-tip conductivity probe (∅=0.025 mm)	L=4.2 m, W=1 m Inflow: uncontrolled broad-crest
		0.075~0.220	0.10				
		0.020~0.08	0.05				

L: chute length; W: chute width

where ΔT as a time scale satisfying: $R_{xy}(T+\Delta T) = 0.5R_{xy}T$; R_{xy} is the normalised cross-correlation function, and Δt is the characteristic time for which the normalised autocorrelation function R_{xx} equals 0.5.

Chord sizes may be calculated from the raw probe signal outputs. The results provide a complete characterisation of the streamwise distribution of air and water chords, including the existence of bubble/droplet clusters. The measurement of air-water interface area is a function of void fraction, velocity, and bubble sizes. The specific air-water interface area a is defined as the air-water interface area per unit volume of air and water. For any bubble shape, bubble size distribution and chord length distribution, it may be derived from continuity: $a=4F/V$ which is valid in bubbly flows ($C<0.3$). In high air content regions, the flow structure is more complex and the specific interface area a becomes simply proportional to the number of air-water interfaces per unit length of flow ($a\propto 2F/V$).

EXPERIMENTAL RESULTS

Basic results

Detailed measurements of void fraction and air-water flow properties were conducted for a number of dimensionless flow rates d_c/h. Identical experiments were repeated with two step sizes in each Channel based upon a Froude similitude (Table 2). Systematic comparisons were performed. Overall the results showed that the distributions of air concentration were properly scaled with a Froude similitude, for the investigated flow conditions (Table 2). This is illustrated in Figs.4 and 5a for Channels 1 and 2 respectively, showing dimensionless distributions of void fraction C where y is the distance normal to the pseudo-bottom formed by the step edges and d_c is the critical flow depth. In addition, the void fraction distributions were compared successfully with an analytical solution of the advection diffusion equation for air bubbles (Chanson and Toombes, 2002). Good agreement was observed further in terms of dimensionless distributions of velocity, as well as in terms of mean air content C_{mean}, dimensionless flow velocity U_w/V_c and air-water flow velocity V_{90}/V_c, where V_{90} is the air-water flow velocity at $y=Y_{90}$, Y_{90} is the characteristic depth where C=0.90, and V_c is the critical flow velocity (Fig.5a).

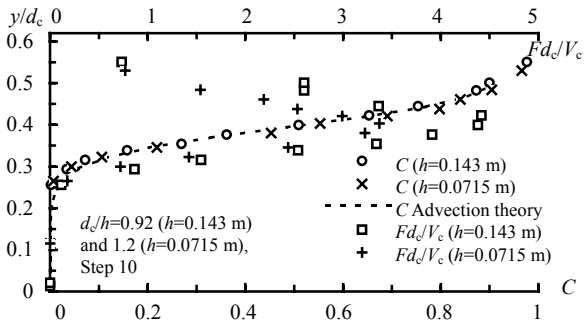

Fig.4 Comparison of dimensionless distributions of void fraction C and bubble count rate Fd_c/V_c in Channel 1 (θ=3.4°, d_c/h~1) for h=0.143 and 0.0715 m. Step 9, x/l=1 (step brink)

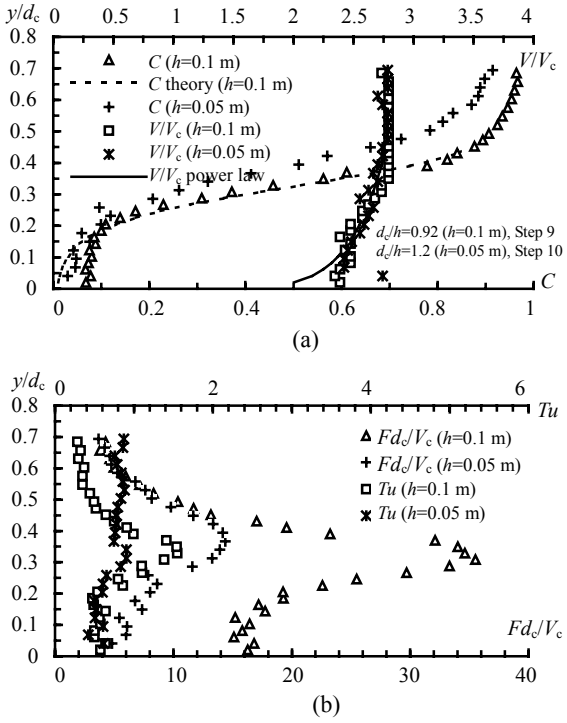

Fig.5 Comparison of dimensionless distributions of void fraction C, bubble count rate Fd_c/V_c, velocity V/V_c and turbulence intensity Tu in Channel 2 (θ=15.9°, d_c/h=1.5) for h=0.10 and 0.05 m at 3 step edges downstream of the inception of free-surface aeration. (a) Dimensionless distributions of void fraction C and velocity V/V_c; (b) Dimensionless distributions of bubble count rate Fd_c/V_c and turbulence intensity Tu

However significant differences, hence scale effects, were observed in terms of dimensionless distributions of bubble count rates Fd_c/V_c and of turbulence intensity Tu as functions of y/d_c where F is the bubble count rate defined as the number of bubbles impacting the probe per second, and d_c and V_c are

the critical flow depth and velocity respectively. In both Channels 1 and 2, lesser dimensionless bubble count rates by about 30% to 50% were observed with the smallest step heights: i.e., h=0.0715 and 0.05 m for θ=3.4° and 15.9° respectively. This is illustrated in Figs.4 and 5b, and the finding implies significant scale effects in terms of number of entrained bubbles and bubble sizes. In Channel 2, differences in turbulence intensity distributions were consistently observed, with lesser maximum turbulence levels for the smallest step height (h=0.05 m). This is illustrated in Fig.5b.

Further, in Channel 2, a comparative analysis of bubble chord size distributions, for similar flow rate, identical location and local void fraction, showed consistently differences between the two step heights: entrained bubbles were comparatively larger in the smallest model (Fig.6a). Figs.6a and 6b present probability distribution functions of air bubble and water droplet chord sizes respectively. Fig.6 compares dimensionless bubble and droplet chord sizes ch/d_c recorded at the same dimensionless distance from the inception point and for the same dimensionless flow rate with two step heights (h=0.1 and 0.05 m). Fig.6a shows dimensionless bubble chord distributions for C=0.10. Fig.6b presents dimensionless droplet chord distributions for C=0.96, at the same cross-sections as in Fig.6a for the two step heights. Basically entrained bubble sizes were not scaled at 2:1 (Fig.6a). A similar observations was made in terms of water droplet size distributions in the spray region (Fig.6b). In dimensional terms, the size distributions of the smallest bubbles and droplets were about the same for both step heights, but a broader range of large particles were seen with the largest step height (h=0.1 m, Channel 2).

Overall the results demonstrated significant scale effects in terms of bubble and droplet size distributions that were not approximated properly by a Froude similitude.

Discussion

The present study was conducted in large-size facilities with large Reynolds numbers between 1.2E+5 and 1.2E+6. The findings of scale effects suggest that physical modelling of stepped chutes based upon a Froude similitude is more sensitive to scale effects than classical smooth-invert chute studies. This is consistent with basic dimensional analysis (Eqs.(1) and (3)) which includes a larger number of relevant parameters, in particular the dimensionless step cavity characteristics.

A basic outcome of the study is the lesser number of entrained bubbles and comparatively greater bubble sizes, as well as lower turbulence levels, observed in the smallest flumes. The findings have direct implications on the flow structure, and on the interactions between turbulence and entrained bubbles. Chanson and Toombes (2002) demonstrated that the air-water flow turbulence level was a function of bubble count rate: $Tu \propto F^{1.5}$. Lesser turbulence levels in small laboratory flumes must imply lesser rate of energy dissipation, particularly on long chutes. That is, small-size models are likely to underestimate the rate of energy dissipation of prototype stepped spillways for similar flow conditions.

Similarly, the lesser number of entrained bubble sizes in laboratory flumes must affect the rate of air-water mass transfer on the chute. Present results imply that the air-water interface area, hence the rate of air-water mass transfer, are underestimated in small-size physical-models. That is, extrapolation

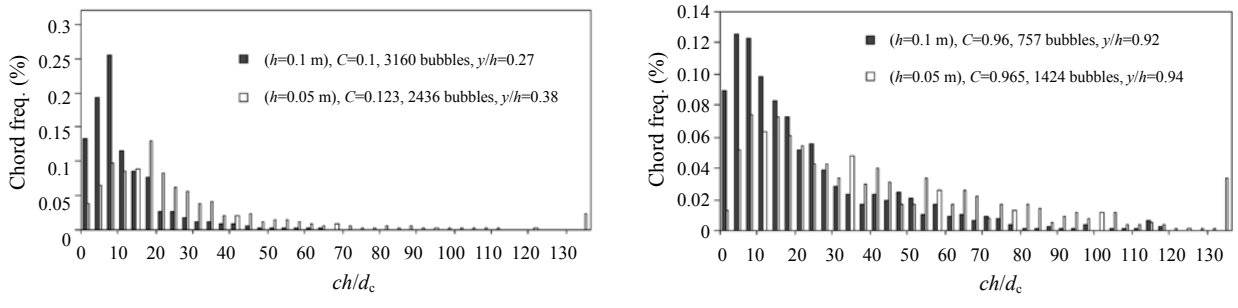

Fig.6 Comparison of dimensionless bubble and droplet chord size ch/d_c distributions in Channel 2 (θ=15.9°, d_c/h=1.5) for h=0.10 and 0.05 m at step edges 9 and 14 respectively

(a) Bubble chord size distributions for C=0.1; (b) Droplet chord size distributions for C=0.96

from small-size models are not reliable, and this may include a wide range of empirical correlations derived from small-size laboratory models.

SUMMARY AND CONCLUSION

The study of stepped chute hydraulics is still based primarily upon physical modelling. It is understood that stepped chute hydraulics is complex because of different flow regimes, strong flow aeration, and interactions between entrained air and turbulence. A complete dimensional analysis yields two basic Eqs.(1) and (3) corresponding respectively to two-dimensional and one-dimensional air-water flows. The analysis emphasises the complexity of stepped chute hydrodynamics, and the limitations of the Froude similitude. Systematic studies of scale effects affecting stepped chute flows are few and the results are sometimes contradictory.

New experimental works were conducted with two slopes and two large step sizes for each large-size facility (Table 2). Identical experiments were performed based upon a Froude similitude with geometrically similar channel configurations. A geometric scaling ratio L_r=2 was used for both invert slopes (θ=3.4° and 16°). Significant scale effects were observed in terms of distributions of bubble count rates, turbulence intensity and bubble/droplet chord sizes. Basically the number of entrained bubble sizes and turbulence levels were drastically underestimated with the smallest step sizes. Further it is demonstrated that the selection of the basic criterion to define scale effects is critical: e.g., flow resistance, air concentration distributions, or turbulence levels.

It is believed that the new results are the first systematic study of scale effects in air-water flows at microscopic scales. The results emphasise that physical modelling of stepped chutes is more sensitive to scale effects than classical smooth-invert chute studies, as demonstrated by dimensional analysis. While the findings were obtained for two moderate slopes (θ=3.4° and 16°), it is thought that the outcomes are valid for a wider range of chute geometry and flow conditions.

References

BaCaRa, 1991. Etude de la Dissipation d'Energie sur les Evacuateurs à Marches. Rapport d'Essais, Projet National BaCaRa, CEMAGREFSCP, Aix-en-Provence, France, p.111 (in French).

Boes, R.M., 2000. Zweiphasenstroömung und Energieumsetzung an Grosskaskaden. Ph.D. Thesis. VAW-ETH, Zürich, Switzerland (in German).

Chamani, M.R., Rajaratnam, N., 1994. Jet Flow on Stepped Spillways. *J of Hyd. Engrg*., *ASCE*, **120**(2):254-259.

Chanson, H., 1994. Hydraulics of nappe flow regime above stepped chutes and spillways. *Aust. Civil Engrg Trans., I. E. Aust*., **CE36**(1):69-76.

Chanson, H., 1997. Air Bubble Entrainment in Free-Surface Turbulent Shear Flows. Academic Press, London, UK, p.401.

Chanson, H., 2001. The Hydraulics of Stepped Chutes and Spillways. Balkema, Lisse, The Netherlands, p.418. http://www.uq.edu.au/~e2hchans/reprints/book4.htm.

Chanson, H., 2002. Air-water flow measurements with intrusive phase-detection probes: Can we improve their interpretation? *J of Hyd. Engrg., ASCE*, **128**(3):252-255.

Chanson, H., 2004. The Hydraulics of Open Channel Flows: An Introduction. Butterworth-Heinemann, Oxford, UK, 2nd Edition. http://www.uq.edu.au/~e2hchans/reprints/book3_2.htm.

Chanson, H., Toombes, L., 2002. Air-water flows down stepped chutes: turbulence and flow structure observations. *Intl J of Multiphase Flow*, **27**(11):1737-1761.

Chanson, H., Toombes, L., 2004. Hydraulics of stepped chutes: the transition flow. *J of Hyd. Res., IAHR*, **42**(1):43-54.

Chanson, H., Yasuda, Y., Ohtsu, I., 2002. Flow resistance in skimming flows and its modelling. *Can J of Civ. Eng*., **29**(6):809-819.

Djenidi, L., Elavarasan, R., Antonia, R.A., 1999. The turbulent boundary layer over transverse square cavities. *J Fluid Mech*., **395**:271-294.

Henderson, F.M., 1966. Open Channel Flow. MacMillan Company, New York, USA.

Knight, D.W., Macdonald, J.A., 1979. Hydraulic resistance of artificial strip roughness. *J of Hyd. Div., ASCE*, **105**(HY6):675-690.

Kobus, H., 1984. Scale Effects in Modelling Hydraulic Structures. Proc. Intl. Symp. on Scale Effects in Modelling Hydraulic Structures, IAHR, Esslingen, Germany.

Lin, K.J., Han, L., 2001. Stepped Spillway for Dachaoshan RCC Dam. *In*: Burgi, P.H., Gao, J.(Eds.), SS2 Key Hydraulics Issues of Huge Water Projects, Proc. 29th IAHR Congress, Special Seminar, Beijing, China, p.88-93.

Minor, H.E., Hager, W.H., 2000. Hydraulics of Stepped Spillways. Proc. International Workshop on Hydraulics of Stepped Spillways. Balkema Publ., Zürich, Switzerland.

Ohtsu, I., Yasuda, Y., 1998. Hydraulic Characteristics of Stepped Channel Flows. *In*: Ohtsu, I., Yasuda, Y.(Eds.), Proc. Workshop on Flow Characteristics around Hydraulic Structures and River Environment. University Research Center, Nihon University, Tokyo, Japan, p.55.

Toombes, L., 2002. Experimental Study of Air-Water Flow Properties on Low-Gradient Stepped Cascades. Ph.D. Thesis, Dept of Civil Engineering, The University of Queensland.

Wood, I.R., 1991. Air Entrainment in Free-Surface Flows. IAHR Hydraulic Structures Design Manual No. 4, Hydraulic Design Considerations. Balkema Publ., Rotterdam, The Netherlands, p.149.